Selective Recognition of Glutathiolated Aldehydes by Aldose Reductase†

Kota V. Ramana,‡ Bharat L. Dixit,‡ Sanjay Srivastava,|| Ganesaratnam K. Balendiran,§ Satish K. Srivastava,‡ and Aruni Bhatnagar*,||

Department of Human Biological Chemistry and Genetics, University of Texas Medical Branch, Galveston, Texas 77555-0647, Department of Cell and Tumor Biology, City of Hope, Medical Center, Duarte, California 91010, Division of Cardiology, Department of Medicine, University of Louisville and the Jewish Heart and Lung Institute, Louisville, Kentucky 40202

Received April 10, 2000; Revised Manuscript Received June 27, 2000

ABSTRACT: In this study, the selectivity and specificity of aldose reductase (AR) for glutathionyl aldehydes was examined. Relative to free aldehydes, AR was a more efficient catalyst for the reduction of glutathiolated aldehydes. Reduction of glutathionyl propanal [γGlu-Cys(propanal)-Gly] was more efficient than that of Gly-Cys(propanal)-Gly and γ-aminobutyric acid-Cys(propanal)-Gly suggesting a possible interaction between α-carboxyl of the conjugate and AR. Two active site residues, Trp20 or Ser302, were identified by molecular modeling as potential sites of this interaction. Mutations containing tryptophan-to-phenylalanine (W20F) and serine-to-alanine (S302A) substitutions did not significantly affect reduction of free aldehydes but decreased the catalytic efficiency of AR for glutathiolated aldehydes. Combined mutations indicate that both Trp20 and Ser302 are required for efficient catalysis of the conjugates. The decrease in efficiency due to W20F mutation with glutathionyl propanal was not observed with γ-aminobutyric-Cys(propanal)-Gly or Gly-Cys-(propanal)-Gly, indicating that Trp20 is involved in binding the α-carboxyl of the conjugate. The effect of the S302A mutation was less severe when γGlu-Cys-(propanal)-Glu rather than glutathionyl propanal was used as the substrate, consistent with an interaction between Ser302 and Gly-3 of the conjugate. These observations suggest that glutathiolation facilitates aldehyde reduction by AR and enhances the range of aldehydes available to the enzyme. Because the N-terminal carboxylate is unique to glutathione, binding of the conjugate with the α-carboxyl facing the bottom of the α/β-barrel may assist in the exclusion of unrelated peptides and proteins.

Aldose reductase (AR)[1] is a cytosolic, $(\alpha/\beta)_8$ barrel protein with a wide tissue and species distribution (for review see refs *1* and *2*). It is a member of the aldo-keto reductase superfamily (AKR1B1; *3*) and catalyzes the reduction of a broad range of aromatic and aliphatic aldehydes, including aldo-sugars. During cellular hyperglycemia AR catalyzes the NADPH-dependent reduction of glucose to sorbitol. Because the cell membrane is relatively impermeable to sorbitol, the progressive osmotic stress due to intracellular sorbitol accumulation has been suggested to be a significant cause of tissue injury and dysfunction associated with long-term diabetes (*1*, *2*, *4*). This view is supported by the observations that inhibition of AR prevents or delays several pleiotropic complications of diabetes such as cataractogenesis, retinopathy, neuropathy, and nephropathy, and in transgenic mice, lens-specific overexpression of AR accelerates sugar cataract (*5*). Nonetheless, the clinical utility of AR inhibitors remains uncertain (*6*, *7*). In several studies, inhibitors of AR do not interrupt or reverse progressive hyperglycemic injury (*7*). Moreover, unlike cataractous lenses, diabetic nerves or kidneys do not accumulate high concentrations of sorbitol (*1*), yet they show functional improvement upon inhibition of AR (*2*, *7*). Thus, a better understanding of the physiological role of AR under normoglycemic and hyperglycemic conditions is essential for critically evaluating the benefits of anti-AR interventions and for assessing the long-term consequences of chronic AR inhibition.

Recent kinetic and structural studies suggest that under normolgycemic conditions, reduction of glucose may be an ancillary role of AR. The purified enzyme displays poor affinity for glucose (K_m = 100 mM), and its active site lacks polar residues required for efficient carbohydrate binding (*8*−*10*). The preferred substrates of the enzyme are aromatic aldehydes (*1*, *10*), isocorticosteroids (*11*), and medium- to long-chain aliphatic aldehydes derived from lipid peroxidation (*10*, *12*). Although, the physiological significance of the reduction of isocorticosteroids and aromatic aldehydes by AR remains to be assessed, the involvement of AR in cellular metabolism of lipid-derived aldehydes has been recently demonstrated. In vitro, AR is an efficient catalyst for the reduction of the lipid peroxidation product 4-hydroxy-*trans*-2-nonenal (HNE) (K_m = 10−30 μM). Moreover, inhibition

† Supported in part by National Institutes of Health Grants DK36118, HL55477, and HL59378.

* To whom correspondence should be addressed: Aruni Bhatnagar, PhD, Division of Cardiology, Department of Medicine, Cardiovascular Research Center, 500 South Floyd, University of Louisville, Louisville, KY 40202. Phone: (502) 852-4883, fax: (502) 852-1795, e-mail: aruni@louisville.edu.

‡ University of Texas Medical Branch.

§ City of Hope Medical Center.

|| University of Louisville and the Jewish Heart and Lung Institute.

[1] Abbreviations: AR, aldose reductase; HNE, 4-hydroxy-*trans*-2-nonenal; DHN, dihydroxynonene; TFA, trifluoroacetic acid; ESI/MS, electrospray ionization/mass spectrometry; DTT, dithiothreiotol; PITC, phenylisothiocynate; DTNB, 5,5′dithiobis(2-nitrobenzoic acid); GSH, reduced glutathione; GS-, glutathionyl; IPTG, isopropyl-β-D-thiogalactoside; HPLC, high-pressure liquid chromatography.

10.1021/bi000796e CCC: $19.00
Published on Web 09/15/2000

of AR alters HNE metabolism in isolated perfused hearts (*13*) and enhances HNE toxicity to vascular smooth muscle cells in culture (*14*). In vivo, feeding AR inhibitors increases the steady-state concentration of HNE in the kidney and the number of apoptotic smooth muscles during vascular inflammation (*15*). Taken together, these observations suggest that reduction and detoxification of lipid-derived aldehydes may be an important normoglycemic function of AR.

Although the active site of AR is compatible with binding and reduction of a wide range of hydrophobic aldehydes (*8*−*10*), the unsaturated aldehydes generated during peroxidation may not be available to AR due to their rapid conjugation to glutathione (*13*). Therefore, in most glutathione-proficient cells, the aldehyde−glutathione adducts rather than the free alkenals are likely to be the endogenous substrates available to AR. Indeed, our studies show that AR is an efficient catalyst for the reduction of aldehyde-glutathione conjugates (*10*, *12*, *14*). Nonetheless, the efficiency and specificity with which the enzyme recognizes these conjugates has not been assessed. In the present paper, we report that glutathione conjugates bind to the AR active site in a specific orientation that enhances the efficiency and the range of aldehydes accessible to AR and minimizes inhibition by unrelated proteins and peptides.

MATERIALS AND METHODS

Materials. Acrolein, propanal, nonanal, *trans*-2-nonenal, *trans*-*trans*-2,4-decadienal, and *trans*-4-decenal were purchased from Aldrich. Glutathione, γGlu-Cys-Glu, NADPH, DL-glyceraldehyde, 5,5′-dithio-bis (2-nitrobenzoic acid; DTNB), DL-dithiothreitol and [^{3}H]-glutathione were purchased from Sigma. Sephadex G-25 (PD-10) columns were purchased from Pharmacia fine chemicals (Uppsala, Sweden). The Gly-Cys-Gly was purchased from Bachem. The HNE was synthesized as its dimethyl acetal from the dimethyl acetal of fumaraldehyde as described previously (*16*). The peptide γ-aminobutyric acid-Cys-Gly was custom synthesized by New England Labs. All other reagents used were of analytical grade.

Synthesis and Purification of Glutathione Conjugates. Reduced glutathione and its analogues were incubated with individual aldehydes in 1:1 mole ratio in 0.1 M potassium phosphate buffer (pH 7.4) at room temperature. The progress of the reaction was monitored by following the decrease in λ_{max} of the aldehydes and by measuring free GSH content by DTNB. The conjugate was purified by HPLC using Rainin reverse phase ODS C_{18} column. The column was preequilibrated with 0.1% TFA in water (solvent A). One milliliter of conjugate (∼ 10 μmol) was injected into the column. The conjugates were eluted using a gradient consisting of solvent A and solvent B (acetonitrile) and monitored at 220 nm. The gradient was generated at 1 mL/min such that solvent B reached 10% in 20 min and 25% in 35 min. The solvent B was then held at 25% for 30 min, after which time its concentration was raised to 60% in 10 min.

Amino Acid Analysis. The conjugates after lyophilization were hydrolyzed in a vapor-phase-automated hydrolyzer (Perkin-Elmer, Foster City, CA). The PTC-amino acids formed after derivatizing with PITC were analyzed using an Applied Biosystems 420/H PTC amino acid analyzer, which is connected to an online 130/A HPLC. The accuracy of the analysis was compared with the standard GSH analyzed under similar conditions.

Table 1: Oligonucleotide Primers for Site-Directed Mutagenesis

mutant	primer
W20F	5′-GCCCTGGAGGGGACTTGAAGGTACCCAACCCCAGG-3′
S302A	5′-CCTTGTGGGAGGTACAGGCCAACAAGGCACAGACC-3′

Electrospray Ionization-Mass Spectrometry (*ESI-MS*). The identity of the GS-aldehyde conjugates was established by ESI-MS using a Micromass ZMD single quadrapole spectrometer. The tuning and calibration solution consisted of poly(ethylene glycol) (PEG2000) in water/methanol (50:50 v/v) containing 0.1% acetic acid. For additional calibration around *m*/*z* 300, GSH was used, which displays a well-resolved peak at *m*/*z* 307. The capillary, the cone, and the extractor were operated at 3.5, 40, and 3 V, respectively, with 40 psi nitrogen at a flow rate of 0.5 L/min. The source block and desolvation temperature were set at 80 and 200 °C, respectively. Typically 1−10 μM solution of the conjugates were prepared in acetonitrile/water/acetic acid (50:50:0.1 v/v/v) and injected into the ion source of the spectrometer using a Harvard syringe pump at a flow rate of 10 μL/min. The mass spectrometer was set to scan from *m*/*z* 100−750 with step size of 0.5, a dwell time of 2 ms, and a scan speed of 45. When dimers of dehydrated ions were observed, the cone voltage and the source block temperature was varied to optimize formation of the parent molecular ion.

Molecular Modeling. The structure of GS-propanal was constructed from the coordinates of GSH (PDB entry 1gra; *17*) and 2-cyclopropylmethylenepropanal (PDB entry 1hrn; *18*), with the starting conformation of GSH the same as that in the crystal structure of glutathione reductase. For AR, the 1.76-Å structure complexed with $NADP^+$ and glucose-6-phosphate was used (PDB entry 2aq; *19*) for the model. The GS-propanal was positioned in the active site of AR using the program O. The aldehyde moiety of GS propanal was positioned such that the carbonyl oxygen of the aldehyde is 2.9 Å from both the NE2 of His110 and the hydroxyl group of Tyr48 and is in the same position as the carboxylate oxygen of zopolrestat (*20*). This resulted in the carbonyl moiety being parallel to the nicotinamide ring of NADPH. Two distinct starting orientations of GS-propanal, termed as orientation 1 and 2, were examined. The propanal group was oriented similarly in both models, and the positioning of the GS-propanal residues γGlu1 and Gly3 were switched in the two models.

Site-Directed Mutagenesis. The QuickChange site-directed mutagenesis kit (Stratagene) was used to construct cDNA sequences encoding tryptophan-to-phenylalanine and serine-to-alanine substitutions at 20 and 302 positions, respectively. The oligonucleotide primers (Table 1) for both strands of the plasmid were custom-synthesized from Sigma Genosys. The pET21D expression vector containing human AR cDNA was used to prepare site-directed mutants, as per the manufacturer's (Stratagene) instructions. First, single mutants of W20F and S302A were prepared, and then a double mutant was constructed using cDNA expressing W20F and oligonucleotide primers for S302A. The identity of the clones containing the desired mutations was confirmed by complete nucleotide sequence analysis. The plasmids encoding wild-

type and mutant AR genes were transfected into BL21(DE3) competent cells (Novagen). The cultures were grown in the presence of ampicillin, and the protein expression was induced by addition of IPTG. The purification of wild-type as well as mutant proteins was carried out as described previously (*21*).

Reduction of the Recombinant Enzymes. Before each experiment, stored proteins were reduced by incubating with 0.1 M DTT at 37 °C for 1 h in 0.1 M potassium phosphate buffer (pH 7.0) containing 1 mM EDTA. Excess DTT was removed by gel filtration over a Sephadex G-25 (PD-10) column, preequilibrated with nitrogen-saturated 0.1 M potassium phosphate buffer (pH 7.0) containing 1 mM EDTA. All the procedures were carried out at 4 °C. The DTT-free, reduced proteins were used within 3 h.

Aldose Reductase Assay. The enzyme activity was measured at room temperature in a 1-mL reaction mixture containing 0.1 M potassium phosphate buffer (pH 7.0), 1 mM EDTA, 10 mM glyceraldehyde, and 0.15 mM NADPH at 25 °C. The reaction was monitored by measuring the disappearance of NADPH at 340 nm, using Varian Cary 100 Bio double beam spectrophotometer. One unit of the enzyme activity is defined as the amount of enzyme required to oxidize 1 μmol of NADPH/min. The control cuvette contained all the components of reaction mixture except the enzyme. The substrate concentration was varied over a range extending from 0.2 to 5−7 times the K_m. Initial velocity was measured at 7−9 different concentrations of each substrate. Individual saturation curves used to obtain k_{cat} and K_m were fitted to a general Michaelis−Menten equation using a nonlinear iterative fitting procedure (*22*).

RESULTS

Docking of the Glutathione Conjugate to the AR Active Site. Our previous studies show that AR catalyzes the reduction of the free aldehydes as well as their glutathione conjugates. To examine the mechanism by which the glutathione conjugate binds to the active site of AR, we modeled the possible orientations of the conjugate at the active site of the enzyme. For this we used an extended form of glutathione, since this has been suggested to be at or near an energy minima. To further constrain the orientation, the aldehyde function of the conjugate was positioned in the hydrophobic cleft with no steric clashes between the substrate and the enzyme, such that its carbonyl oxygen retains the geometry described for the carboxylate of the active site inhibitor zopolrestat. As shown in Figure 1, two distinct orientations of the glutathione conjugate are possible at the AR active site, without a change in the geometry of propanal group. The sulfur atom of GS-propanal is within 5 Å of the sulfur atom of Cys298. In both orientations, multiple interactions between the glutathionyl backbone of the conjugate and polar residues of the AR active site are possible. In orientation 1, the N-terminal end of the conjugate faces the bottom of the barrel, with selective hydrogen-bonding between Lys21(NE1), Trp 20(NE1), and O11 of Glu1 of the conjugate. Additionally, Val47-O could form a hydrogen-bond with N1 of Glu1. The Gly3 of the conjugate faces the lip of the barrel and is within bonding distance of the residues Ser302-N and Leu301-N. In contrast, in orientation 2, the α-carboxylate group of Glu1 is at the lip of the barrel, whereas Gly3 at the C-terminal of the conjugate faces downward. In this orientation, the Glu1-O11 of the conjugate is within bonding distance of Ser302-OG and Glu1-O12 could hydrogen bond with Ser302-N and Ser302-OG. The Gly3 could form hydrogen bonds with the active site residues Trp20, Val47, and Tyr48. Because in both orientations the binding of the conjugate to the active site could be stabilized by multiple hydrogen bonds, it is difficult to readily predict which of the two orientations represents the preferred mode of binding to the active site. Hence, we generated site-directed mutants in which the two key binding residues, Trp20 or Ser302, were substituted with related amino acids in which the expected hydrogen bonds will not be formed and examined the steady-state kinetic parameters of these mutants with aldehyde conjugates of glutathione and its analogues.

Steady-State Kinetic Properties of AR and Site-Directed Mutants with Free Aldehydes. The WT AR and its site-directed mutants W20F, S302A, and W20F + S302A displayed identical molecular weight bands on SDS−PAGE and Western blots were stained by anti-AR antibodies (data not shown). The steady-state kinetic parameters of the WT and mutant forms of AR were determined using DL-glyceraldehyde, acrolein, or HNE as the variable substrate. In agreement with previous measurements (*10*), WT AR reduced HNE and glyceraldehyde with high catalytic efficiency, whereas reduction of acrolein was 10-fold less efficient. Nonetheless, no significant differences were observed between the WT AR and its site-directed mutants in the K_m or the k_{cat}/K_m values for these aldehydes (Table 2). However, a slightly lower catalytic efficiency of W20F and S302A was observed with HNE as the substrate, although the efficiency for the reduction of HNE by WT AR and the double mutant (W20F + S302A) was comparable. From these data, we infer that the residues Ser302 and Trp20 do not play a significant role in binding or catalysis of free aldehyde substrates of varying chain length.

Reduction of Glutathione Conjugates by AR and Site-Directed Mutants. Since no significant changes in the reduction of free aldehydes were observed, we examined whether the residues Ser302 and Trp20 selectively participate in binding of glutathione conjugates. For this series of experiments, conjugates of acrolein, *trans*-2-nonenal and *trans-trans*-2,4-decadienal, and glutathione were synthesized as described under Materials and Methods. The purified conjugates, glutathionyl propanal, nonanal, and *trans*-4-decenal, formed single well-resolved ions upon ESI^+/MS. The *m*/*z* values of these ions were 364.4, 448.3, and 460.4, respectively (data not shown). These values are ± 0.2 of the expected *m*/*z* values of the $[M + H]^+$ ions of 1:1 adducts between glutathione and the aldehyde, indicating that these conjugates are simple Michael adducts between the thiol of glutathione and the C-3 electron deficient center of the α,β-unsaturated aldehydes. No molecular ions corresponding to a 1:2 adduct or a Schiff base were observed. For measurement of AR activity, the synthesized conjugates were appropriately diluted. Under these conditions, no significant dissociation of the conjugates was observed. Since conjugation removes unsaturation, the kinetic parameters obtained for the reduction of the conjugates were compared with those for the corresponding free aldehydes saturated at C-3, propanal, nonanal, and *trans*-4-decenal. As shown in Table 3,

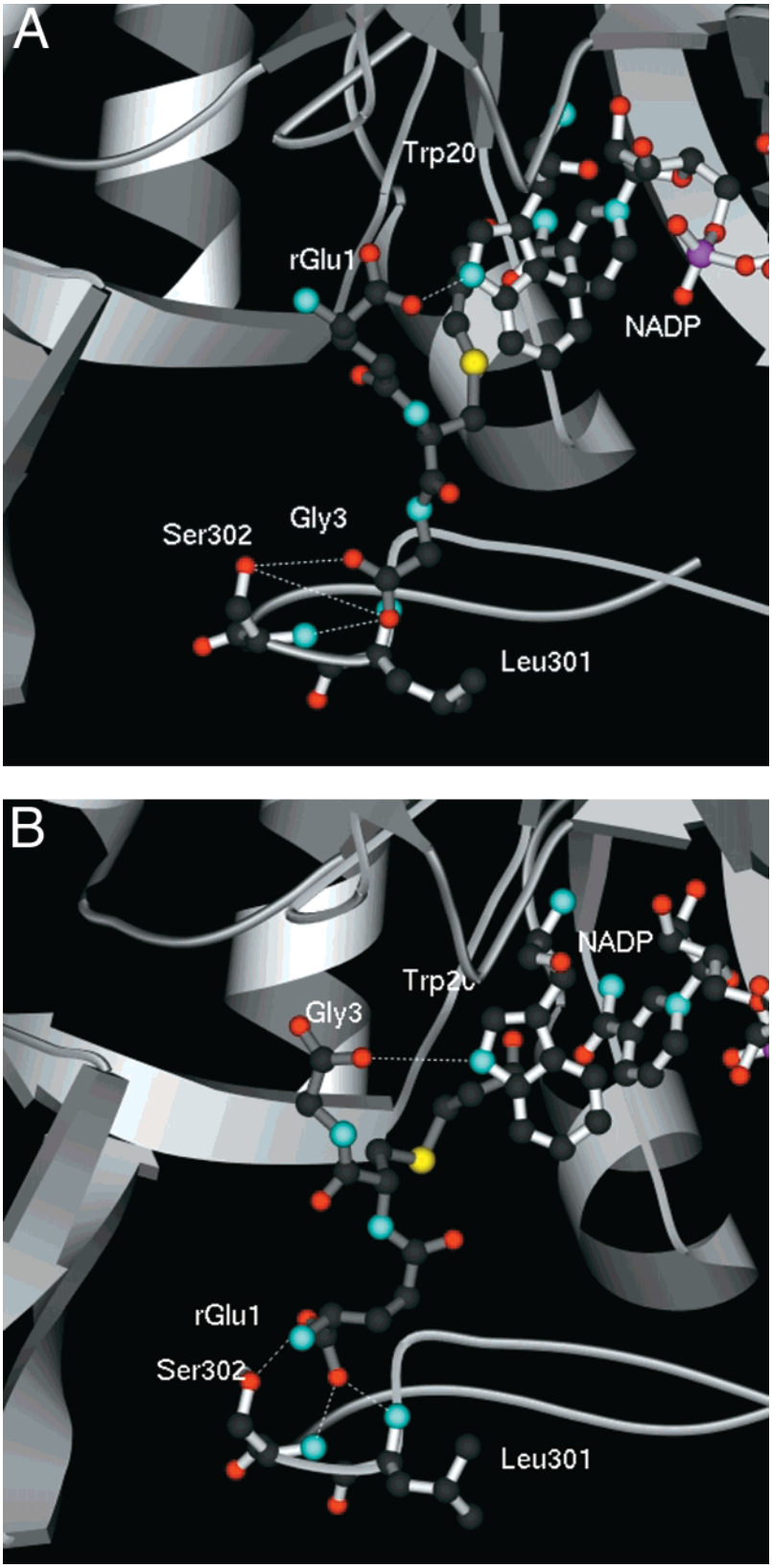

FIGURE 1: Ribbon representation of the active site of aldose reductase bound to glutathionyl propanal and NADPH. The α-carbon backbone of the enzyme is shown in gray. Glutathionyl propanal and NADPH are drawn as ball-and-stick models. Potential hydrogen bonds are shown as dashed white lines. Carbon atoms of the ligands shown in dark gray, and nitrogen, oxygen, and sulfur are colored blue, red, and yellow, respectively. Two possible orientations are shown. In orientation 1 (panel A), γGlu1 of the conjugate is within bonding distance of Trp20 and Gly3 could potentially interact with Ser302 and Leu301. In orientation 2 (panel B) possible interactions between Gly3 and Trp20 and γGlu1 and Ser302 and Leu301 are shown. The figure was drawn using MOLSCRIPT.

AR displayed consistently higher catalytic efficiency with the glutathione conjugates as compared to the free aldehydes. The maximal increase in catalytic activity was for glutathionyl propanal, in which case the k_{cat}/K_m increased 700-fold, with a 200-fold lower K_m. Although the values of the kinetic constants for the glutathione conjugates are similar to those

Table 2: Steady-State Kinetic Parameters for Wild-Type (WT) and Mutant W20F, S302A, and W20F + S302A Forms of Human Aldose Reductase[a]

	K_m (μM)				k_{cat} (min^{-1})				K_m/k_{cat} (min^{-1}/mM^{-1})			
substrate	WT	W20F	S302A	W20F + S302A	WT	W20F	S302A	W20F + S302A	WT	W20F	S302A	W20F + S302A
DL-glyceraldehyde	48	51	54	56	26.5	28.9	35.4	35.4	552	567	656	632
acrolein	880	711	772	703	43.7	40.3	36.1	48.5	50	57	47	69
4-hydroxy-*trans*-2-nonenal	31	28	33	35	36.4	22.4	27.9	36.0	1174	800	845	1029

[a] Kinetic parameters were determined in 0.1 M potassium phosphate containing 1 mM EDTA, 150 μM NADPH, and varied concentrations of the aldehyde; standard deviation < 20%.

Table 3: Steady-State Kinetic Parameters for the Reduction of Aldehydes and Aldehyde−Glutathione Conjugates by Wild-Type (WT) and Mutant W20F, S302A, and W20F + S302A Forms of Human Aldose Reductase[a]

	K_m (μM)				k_{cat} (min^{-1})				k_{cat}/K_m (min^{-1}/mM^{-1})			
substrate	WT	W20F	S302A	W20F + S302A	WT	W20F	S302A	W20F + S302A	WT	W20F	S302A	W20F + S302A
propanal	6370	6450	4990	11 000	26.0	25.6	21.6	24.4	4.1	4.0	4.3	2.2
GS-propanal	30	350	230	620	91.5	127.7	143.3	117.5	3050	365	623	190
nonanal	22	20	24	22	22.0	22.9	24.6	25.2	1000	1145	1025	1146
GS-nonanal	4.5	29	18	74	16.0	22.8	18.7	27.0	3556	786	1039	365
trans-4-decenal	68	53	48	44	21.6	22.2	19.9	20.7	318	419	415	471
GS-*trans*-decenal	10.0	75	43	105	16.9	27.5	25.9	24.5	1690	367	602	233

[a] Glutathione conjugates were synthesized by reacting unsaturated aldehydes with reduced glutathione, purified and quantified as described in the text. Since conjugation removes unsaturation, the kinetic constants obtained with the conjugates are compared with the corresponding free saturated aldehyde; standard deviation < 20%.

reported earlier (*10*), slight differences were noted, presumably due to lower NADPH concentrations in the assay buffer used earlier (*10*). Nonetheless, under identical reaction conditions, significantly higher catalytic efficiencies (k_{cat}/K_m) were also observed with the glutathionyl nonanal and glutathionyl *trans*-4-decenal as compared to the free aldehyde, indicating that in comparison to the free aldehydes, glutathione conjugates are better substrates of AR.

An enhancement of catalytic efficiency due to glutathiolation was also apparent when W20F:AR and S302A:AR were used as catalysts for the reduction of propanal and glutathionyl propanal. However, as compared to a 700-fold increase in k_{cat}/K_m observed with the WT AR, this difference was only 90- to 150-fold for these site-directed mutants. Since the parameters for the reduction of propanal were not affected by S302A and W20F substitutions, these observations suggest that the Ser302 and Trp20 are involved in binding of the glutathionyl conjugate but not free propanal. The critical role of Ser302 and Trp20 in binding the glutathione backbone of the aldehyde conjugates is also apparent from comparisons of the catalytic efficiencies of nonanal and *trans*-4-decenal with their corresponding glutathione conjugates. While glutathiolation enhanced the efficiency with which WT AR catalyzes the reduction of nonanal and *trans*-4-decenal, no significant enhancement in efficiency was observed with W20F:AR and S302A:AR. Moreover, the catalytic efficiency of the double mutant with the glutathione conjugates of nonanal and *trans*-4-decenal was lower than with free aldehydes. In all the cases, the increase in the K_m or decrease in k_{cat}/K_m was in the order of W20F + S302A > W20F > S302A (Table 3). Thus, collectively, these data indicate that Ser302 and Trp20 are critical determinants of the catalytic efficiency of the enzyme for the reduction of glutathione conjugates but not the free aldehydes.

Reduction of Conjugates of Glutathione Analogues. To assess the contribution of individual amino acid residues of glutathione, reduction of the propanal conjugates of three glutathione analogues by AR and its site-directed mutants was examined. The propanal conjugates of γGlu-Cys-Glu, Gly-Cys-Gly, and γ-aminobutyric acid-Cys-Gly were synthesized and purified as described under Materials and Methods. Upon ESI$^+$/MS, the *m*/*z* values obtained for these conjugates were 435.3, 292.2, and 319.2, respectively, indicating that like glutathione, these peptides form a 1:1 adduct with acrolein but do not form Schiff bases. The reduction of propanal conjugates of these peptides was catalyzed by WT AR with variable efficiency. Substitution of the C-terminal Gly with Glu did not decrease the catalytic efficiency of the enzyme. In fact, γGlu-Cys(propanal)-Glu was reduced more efficiently by WT AR than glutathionyl propanal, indicating that the presence of an additional negative charge at the C-terminus of the conjugate facilitates catalysis. However, the propanal conjugate of the peptide in which the γGlu of glutathione was replaced by Gly [Gly-Cys (propanal)Gly] was reduced less efficiently by WT AR (Table 4), suggesting that the Glu1 residue of glutathione may be important in binding of the conjugate to the active site of the enzyme. That this is partially due to the α-carboxyl group of Glu1 is indicated by the lower catalytic efficiency of the enzyme with γ-aminobutyric-Cys-(propanal)-Gly as compared to glutathionyl propanal.

As with the glutathionyl propanal, the reduction of γGlu-Cys(propanal)-Glu was less efficient when W20F:AR or S302A:AR was used as catalysts instead of WT AR. However, the efficiency for the reduction of γGlu-Cys-(propanal)-Glu by S302A:AR was 67% of that observed with the WT enzyme, as compared to efficiency for reduction of glutathione propanal which was 20% of that of WT AR. The less severe decrease in the reduction of γGlu-Cys(propanal)-Glu as compared to glutathionyl propanal suggests a potential interaction between Ser302 and Gly3 of glutathione propanal at the AR active site. The decrease in the catalytic efficiency of the W20F:AR as compared to WT AR was comparable

Table 4: Steady-State Kinetic Parameters for the Reduction of Aldehyde Conjugates of Glutathione and Analogs by Wild-Type (WT) and Mutants W20F, S302A, and W20F + S302A Forms of Human Aldose Reductase[a]

	K_m (μM)				k_{cat} (min^{-1})				k_{cat}/K_m (min^{-1}/mM^{-1})			
propanal conjugate	WT	W20F	S302A	W20F + S302A	WT	W20F	S302A	W20F + S302A	WT	W20F	S302A	W20F + S302A
γGlu-Cys-Gly	30	350	230	620	91.5	127.7	143.3	117.5	3050	365	623	190
γGlu-Cys-Glu	19	260	21	267	71.4	150.0	52.7	99.7	3758	577	2510	373
Gly-Cys-Gly	50	46	33	52	97.2	120.9	51.6	71.2	1944	2628	1564	1369
γ-amino-butyric acid-Cys-Gly	38	46	40	50	91.5	94.9	55.0	53.6	2408	2063	1375	1072

[a] Propanal conjugates of glutathione and analogues were prepared as described in the text; standard deviation < 20%.

when either glutathionyl propanal or γGlu-Cys(propanal)-Glu was used as the substrate, showing that substitution of the C-terminal glycine of the conjugate with Glu does not alter its efficacy as a substrate of AR. This is consistent with the binding mode of the conjugate in which the N-terminal Glu1, rather than the C-terminal Gly3 of the conjugate, interacts with Trp20. As indicated above, deletion of the free N-terminal carboxyl group of the conjugate appeared to decrease the catalytic efficiency with which it is reduced by the WT enzyme. However, k_{cat}/K_m of γ-aminobutyric acid-Cys-(propanal)-Gly was not different from that of W20F:AR, although the conjugate was reduced less efficiently by S302A:AR than the WT AR. These observations suggest that deletion of the α-carboxyl group of Glu1 does not affect the decrease in efficiency observed with the S302A mutation, while it annuls the consequences of the W20F mutation, suggesting a specific interaction between Trp20 but not Ser302 with the α-carboxyl of Glu1 of the conjugate. This mode of binding is consistent with orientation 1 (Figure 1).

DISCUSSION

Despite extensive investigations, the physiological function(s) of AR remains unclear. Our previous studies show that AR is a more efficient catalyst for the reduction of medium-chain hydrophobic aldehydes than aldoses, suggesting that the enzyme may be involved in the metabolism and detoxification of lipid peroxidation products (*10*). Several of the aldehydes derived from lipid peroxidation are, however, strongly electrophilic and readily conjugate with glutathione to form Michael adducts (*23*). That these adducts are reduced by AR in vivo is demonstrated by our observation that the formation of glutathionyl dihydroxynonene (GS-DHN) from HNE is inhibited in the rat hearts perfused with the AR inhibitor, sorbinil (*13*). Nevertheless, the specificity of AR for glutathione−aldehyde adducts has not been assessed. Moreover, it remains unclear how, despite a highly hydrophobic active site, the enzyme catalyzes the reduction of hydrophilic glutathione conjugates with high efficiency. Thus, to gain further insight into the mechanism by which AR catalyzes the reduction of glutathione conjugates, we examined potential interactions between glutathione and the active site residues of AR. Our molecular modeling studies show that the constraints placed on the glutathione binding by the high hydrophobicity of the active site could be overcome by the interactions of the conjugate and the scant, but appropriately located, residues surrounding the active site. The critical ionizable polar residues at the active site of AR are His110, Tyr48, and Cys298. However, none of the residues could directly interact with the glutathione backbone of the conjugate. The residues His-110 (*20*) and Tyr-48 (*19*, *24*) are expected to form hydrogen bonds with carbonyl of aldehyde substrate, and Cys298 is located too close to the NADPH ring (*9*) to provide significant anchoring to glutathione conjugates. The active site of the enzyme is, however, large—12 Å deep and 7 × 13 Å wide—and could readily accommodate glutathiolated aldehydes, depending upon the conformation of the protein-bound glutathione. For our studies, we used an extended form of the glutathione molecule. Although in solution and in crystals glutathione adopts a folded conformation, it usually binds in an extended form to most glutathione binding proteins such as glyoxalase I, T4 glutaredoxin, glutathione peroxidase and reductase, and π class glutathione *S*-transferases (*25*−*29*).

When modeled with the glutathione in the extended form and the aldehyde carbonyl is constrained to the geometry expected of the substrate, two distinct orientations of the molecule were suggested. As shown in Figure 1, these orientations differ in the position of the glutathione backbone. In orientation 1, the N-terminus faces the bottom of the barrel with Gly3 of the conjugate interacting with Ser302 and Leu301 and the γGlu1 of the conjugate close to Trp20 and Val 47. The alternative model (orientation 2) places the γGlu1 within hydrogen bonding distance of Ser302 and Leu301 and Gly3 close to Val47. To distinguish between these possibilities, and to assess whether binding of the conjugate in a specific orientation is required for optimal catalysis, we systematically altered the amino acid residues of the glutathione backbone as well as the active site and measured changes in the steady-state kinetics of the enzyme with free aldehydes and their thiol conjugates.

The catalytic efficiencies of the enzyme with different substrates and its site-directed mutants were compared using the steady-state parameter k_{cat}/K_m. In case of AR, the values of K_m do not correspond to a unitary rate constant and are not a direct measure of substrate binding (*1*, *30*, *31*). Because the overall rate of the catalytic cycle is limited by the slow isomerization of the binary complex (E:NADP), k_{cat} values reflect the rate of release of the oxidized nucleotide and are relatively insensitive to the aldehyde binding and catalysis. However, analysis of the reaction scheme shows that k_{cat}/K_m of the aldehyde substrate corresponds to the unitary on-rate constant of the aldehyde binding to enzyme (*10*) and provides a measure of relative catalytic efficiencies under similar reaction conditions that show small changes in k_{cat}. As expected, the catalytic efficiency of AR was not severely affected by mutations at positions 20 and 302, indicating that these changes do not cause gross perturbation in the protein structure and do not severely affect the binding or catalysis of free aldehydes. Nonetheless, as compared to the WT enzyme, slightly lower catalytic efficiencies of W20F:

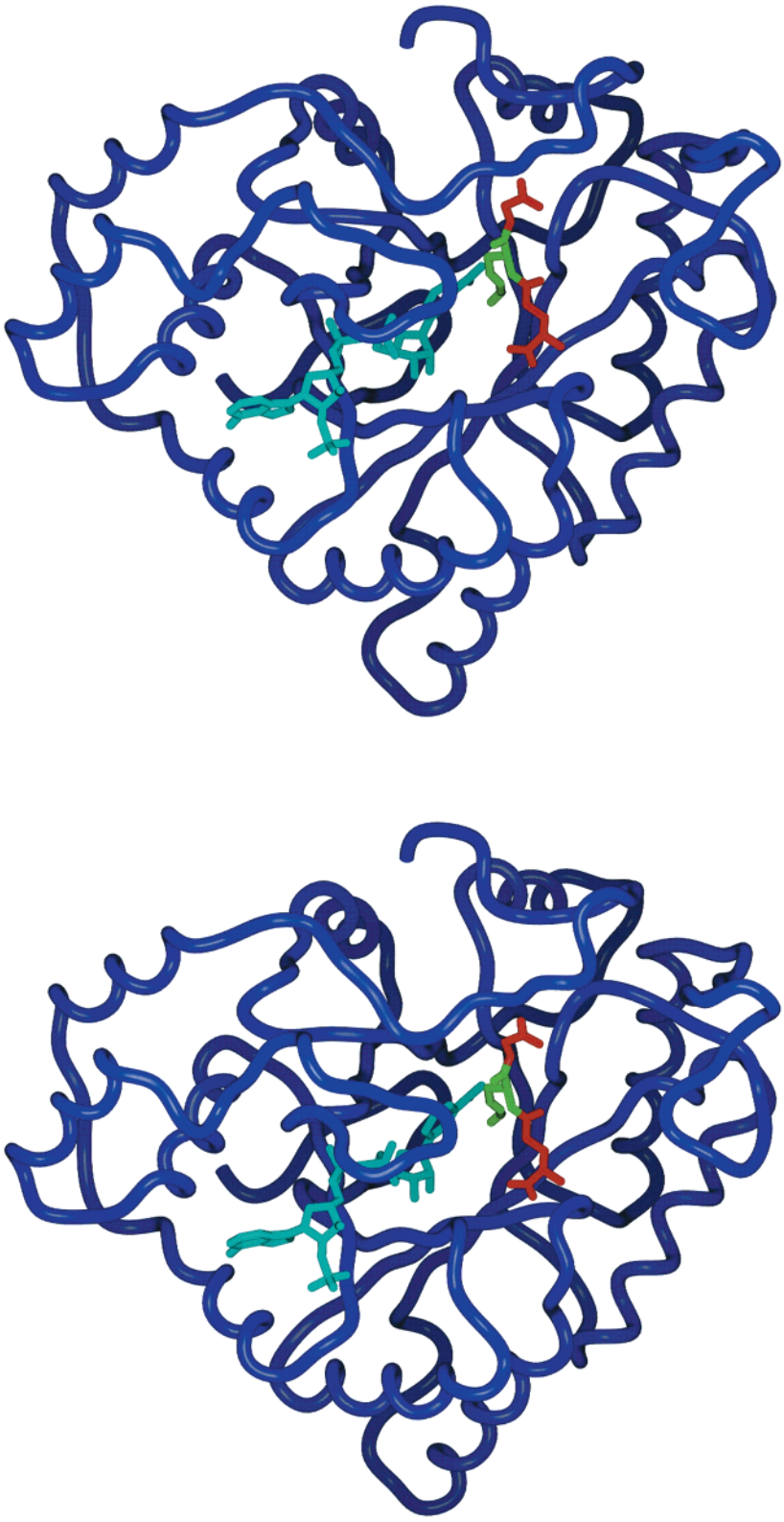

FIGURE 2: Stereo perspective view of the α-carbon backbone trace of the structure of aldose reductase with glutathionyl propanal and NADPH bound to the active site. The glutathionyl propanal and NADPH are drawn as stick models. NADPH is shown in cyan, Cys-propanal is colored green, and the glycine and glutamate are shown in red. The molecule is viewed down the C-terminus of the β-barrel, and the conjugate is oriented with its N-terminus facing the bottom of the barrel, and the carbonyl of propanal is constrained to the orientation adopted by the carboxylate of the active site inhibitor zopolrestat (*20*). The figure was drawn using MOLSCRIPT.

AR and S302A:AR were observed with HNE as the substrate. As suggested by our previous studies (*10*), C_4-C_5 gauche conformation of nonenal, with an otherwise all anti conformation, results in the C_4 and C_5 methylene groups in contact with Trp20 and the C_8 and C_9 methylene groups in contact with Leu301, which with the 4-OH derivative of nonenal could interact with Ser302. Thus, substitution of Trp20 could affect the binding of aldehydes with >4 carbons, whereas a mutation at Ser302 could alter the binding of aldehydes with >8 carbons. This is consistent with our present data showing

that W20F and S302A mutations selectively affect the kinetic parameters of the C-9 aldehyde (HNE) but not the C-3 aldehydes (glyceraldehyde and acrolein). The comparable catalytic efficiencies of the WT enzyme and W20F + S302A:AR suggest that in the double mutant, both the medial and the distal interactions are altered, allowing a more relaxed fit of the aldehyde at the active site.

In all the cases examined, a comparison of catalytic efficiencies of WT AR with free and glutathiolated aldehydes reveals that glutathiolation enhances the efficiency of the enzyme (Table 3), indicating that the glutathione conjugates are better substrates of AR than the corresponding unconjugated aldehydes. The increase in catalytic efficiency due to glutathiolation was, however, dependent on the structure of the parent aldehyde. Greater enhancement was observed by the C-3 aldehyde (700-fold) than with C-9 or C-10 aldehydes (3−5-fold). Thus, it may appear that the catalytic advantage conferred by glutathiolation may be simply a matter of size. Since the conjugate is larger than the aldehyde, it interacts more extensively with the active site residues via hydrophobic/van der Waal interactions. However, the observation that the catalytic advantage could be abrogated by substitutions at positions 20 and 302 of AR indicates that selective hydrogen bonds rather than nonselective hydrophobic interactions mediate recognition of the conjugate at the AR active site. Indeed, the glutathione conjugates of aldehydes were reduced by W20F + S302A:AR with an efficiency that was between 6 and 13% of WT AR, even though the catalytic efficiency for the reduction of the free aldehyde was not significantly affected. Furthermore, the 3−5-fold catalytic advantage due to glutathiolation, observed with the WT AR with C-9 and C-10 aldehydes was overcome by these mutations indicating a critical role of Trp20 and Ser302 in orienting and/or recognition of the glutathione conjugate at the AR active site.

Specific recognition and binding of glutathione at the AR active site is further supported by the results of our experiments with these site-directed mutants and glutathione analogues. In general, these results show that Trp20 plays a more critical role in orienting and binding of the glutathione conjugate than Ser302, because as compared to WT AR, the kinetic efficiency of W20F:AR was more severely affected than that of S302A:AR. Additionally, our data suggest that Trp20 stabilizes the conjugate by interacting with the carboxyl group of γGlu1 of the conjugate. The significance of the Trp20−Glu1 interaction is underscored by the observation that the decrease in catalytic efficiency due to the W20F mutation observed with glutathionyl propanal was not evident when γ-aminobutyric acid-Cys(propanal)-Gly was used as a substrate. Thus in the absence of the α-carboxylate (in the γ-aminobutyric acid analog) both the WT and the W20F:AR catalyze the reduction of the conjugate with comparable efficiencies, suggesting specific interaction between Trp20 the α-carboxylate of Glu1. That Glu1 interacts with Trp20 is also suggested by the observation that the reduction of Gly-Cys(propanal)-Gly by W20F:AR was more efficient than by the WT enzyme, whereas W20F:AR was a poor catalyst for the reduction of γGlu-Cys(propanal)-Glu. This observation also rules out a possible interaction between Gly3 of the conjugate and Trp20 of AR, since this interaction would predict that γGlu-Cys(propanal)-Glu should be reduced as efficiently by W20F AR as WT AR. Because this was not observed, we infer that Gly3 does not interact with Trp20. Conversely, our experiments suggest that Gly3 of the conjugate interacts with Ser302 of AR. This interaction is suggested by the observation that although the catalytic efficiency of S302A:AR was 20% of the WT enzyme, with glutathionyl propanal as the substrate, the efficiency of this mutant was 70% of WT AR when γ-Glu-Cys(propanal)-Glu was the substrate, indicating that removal of Gly3 overcomes the loss of efficiency due to the Ser302A mutation. Thus, together these data are consistent with the binding of the conjugate to the AR active site in orientation 1 and suggest that the conjugate binds to AR with its N-terminal facing the bottom of the barrel (Figure 2).

The N-terminal α-carboxylate is a motif unique to glutathione and is selectively recognized by most glutathione binding proteins. Although glutathione binding enzymes such as T4 glutaredoxin (*32*) and glutathione S-transferases (*33*) form contacts with other residues of glutathione, proteins such as glyoxalase (*25*) and glutathione reductase (*26*) show predominant or exclusive recognition of the N-terminus of the peptide with little or no specific interaction with Gly3. Thus dominant interaction of AR via the glutamyl end of glutathione suggests an adaptation analogous to glyoxalase and glutathione reductase. This interaction may also help the enzyme in discriminating between glutathione and other peptides. Should AR bind to the conjugate in orientation 2, with the C-terminal glycine inside the β-barrel, the active site of the enzyme is more likely to be occupied by unrelated proteins and peptides with similar C-termini. It is also significant that the glutathione binding site of AR is defined by residues located at the two ends of the amino acid sequence (20 and 302), which suggests that the entire architecture of the protein rather than a subsidiary domain, is involved in glutathione binding.

The high catalytic efficiency of AR with glutathione−aldehyde conjugates suggests that the glutathiolation enhances the range of aldehydes accessible to AR. Previous studies show that the AR is particularly efficient at reducing unbranched saturated and unsaturated medium chain aldehydes, with carbon chain lengths varying from five to nine. Aldehydes with carbon chains less than five or more than nine are reduced less efficiently. Presumably due to decreased flexibility, the catalytic efficiency also decreases with increased unsaturation (e.g., the k_{cat}/K_m values for the series, hexanal, *trans*-2-hexenal, and *trans-trans*-2,4-hexadienal are 3660, 220 and 140; ref *10*). Thus, glutathiolation by removing unsaturation and providing additional specific interactions with the active site residues converts aldehydes to a form more suitable for AR and in essence recruits aldehydes that would otherwise escape reduction by this enzyme.

REFERENCES

1. Bhatnagar, A., and Srivastava, S. K. (1992) *Biochem. Med. Metabol. Biol. 48*, 91−121.
2. Yabe-Nishimura, C. (1998) *Pharmacol. Rev. 31*, 21−33.
3. Jez, J. M., Bennett, M. J., Schlegel, B. P., Lewis, M., and Penning, T. M. (1997) *Biochem. J. 326*, 625−636.
4. Kador, P. F., Robinson Jr., W. G., and Kinoshita, J. H. (1985) *Annu. Rev. Pharmacol. Toxicol. 25*, 691−714.
5. Lee, A. Y., Chung, S. K., and Chung, S. S. (1995) *Proc. Natl. Acad. Sci. U.S.A. 92*, 2780−2784.
6. Parry, G. J. (1999) *Am. J. Med. 107*, 27S−33S.

7. Sarges, R., and Oates, P. J. (1993) *Prog. Drug Res. 40*, 99−161.
8. Rondeau, J. M., Tete-Favier, F., Podjarny, A., Reymann, J. M., Barth, P., Biellmann, J. F., and Moras, D. (1992) *Nature 355*, 469−472.
9. Wilson, D. K., Bohren, K. M., Gabbay, K. H., and Quiocho, F. A. (1992) *Science 257*, 81−84.
10. Srivastava, S., Watowich, S. J., Petrash, J. M., Srivastava, S. K., and Bhatnagar, A. (1999) *Biochemistry 38*, 42−54.
11. Wermuth, B., and Monder, C. (1983) *Eur. J. Biochem. 131*, 423−426.
12. Vander Jagt, D. L., Kolb, N. S., Vander Jagt, T. J., Chino, J., Martinez, F. J., Hunsaker, L. A., and Royer, R. E. (1995) *Biochim. Biophys. Acta 1249*, 117−126.
13. Srivastava, S., Chandra, A., Wang. L., Seifert Jr., W. E., DaGue, B. B., Ansari, N. H., Srivastava, S. K., and Bhatnagar, A. (1998) *J. Biol. Chem. 273*, 10893−10900.
14. Spycher, S. E., Tabataba-Vakili, S., O'Donnell, V. B., Palomba, L., and Azzi, A. (1997) *FASEB J. 11*, 181−188.
15. Rittner, H. L., Hafner, V., Klimiuk, P. A., Szweda, L. I., Goronzy, J. J., and Weyand, C. M. (1999) *J. Clin. Invest. 103*, 1007−1013.
16. Chandra, A., Srivastava, S. K. (1997) *Lipids 32*, 779−782.
17. Becker, K., Savvides, S. N., Keese, M., Schirmer, R. H., and Karplus, P. A. (1998) *Nat. Struct. Biol. 5*, 267−271.
18. Tong, L., Pav, S., Lamarre, D., Pilote, L., LaPlante, S., Anderson, P. C., and Jung, G. (1995) *J. Mol. Biol. 250*, 211−222.
19. Harrison, D. H., Bohren, K. M., Ringe, D., Petsko, G. A., and Gabbay, K. H. (1994) *Biochemistry*, *33*, 2011−2020.
20. Wilson, D. K., Tarle, I., Petrash, J. M., and Quiocho, F. A. (1993) *Proc. Natl. Acad. Sci. U.S.A. 90*, 9847−9851.
21. Petrash, J. M., Harter, T. M., Devine, C. S., Olins, P. O., Bhatnagar, A., Liu, S., and Srivastava, S. K. (1992) *J. Biol. Chem. 267*, 24833−24840.
22. Cleland, W. W. (1979) *Methods Enzymol. 63*, 103−138.
23. Esterbauer, H., Schaur, R. J., and Zollner, H. (1991) *Free Rad. Biol. Med. 11*, 81−128.
24. Bohren K. M., Grimshaw, C. E., Lai, C. J., Harrison, D. H., Ringe, D., Petsko, G. A., and Gabbay, K. H. (1994) *Biochemistry* 33, 2021−2032.
25. Cameron, A. D., Olin, B., Ridderstorm, M., Mannervik, B., and Jones, T. A. (1997) *EMBO J. 16*, 3386−3395.
26. Karplus, P. A., Pai, E. F., and Schultz, G. E. (1989) *Eur. J. Biochem. 178*, 693−703.
27. Nordstrand, K., Slund, F., Holmgren, A., Otting, G., and Berndt, K. D. (1999) *J. Mol. Biol. 286*, 541−552.
28. Ridderstrom, M., Cameron, A. D., Jones, T. A., and Mannervik, B. (1998) *J. Biol. Chem. 273*, 21623−21628.
29. Epp, O., Ladenstein, R., and Wendel, A. (1983) *Eur. J. Biochem. 133*, 51−69.
30. Grimshaw, C. E., Bohren K. M., Lai, C. J., Gabbay, K. H. (1995) *Biochemistry 34*, 14356−14365.
31. Grimshaw, C. E. (1992) *Biochemistry 31*, 10139−10145.
32. Nikkola, M., Gleason, F. K., Saarinen M., Joelson, T., Bjornberg O., Eklund, H. (1991) *J. Biol. Chem.* 266, 16105−16112.
33. Ji, X., von Rosenvinge E. C., Johnson, W. W., Armstrong, R. N., Gilliland, G. L. (1996) *Proc. Natl. Acad. Sci. U.S.A. 93*, 8208−8213.

BI000796E